FAST SWITCHING BEHAVIOUR OF NANOSCOPIC NiFe- AND Co-ELEMENTS

J. Fidler, T. Schrefl, V.D. Tsiantos, W. Scholz and D. Suess
Institute of Applied and Technical Physics, Vienna University of Technology

Wiedner Hauptstr. 8-10, A-1040 Vienna, Austria

Abstract

Three-dimensional micromagnetic simulations were performed to study the magnetisation reversal processes of granular nanoelements using a hybrid finite element/boundary element model. Transient magnetisation states during switching are investigated numerically in granular, thin $Ni_{80}Fe_{20}$ and Co square shaped nanoelements (100 x 100 nm^2) with 10 nm grain size and a thickness of 10 nm and taking into account a random orientation of the grains. Switching dynamics are calculated for external fields between 80 kA/m and 280kA/m, which were uniformly applied after a rise time of 0.05 and 0.1 ns, respectively, and in comparison for a 10 GHz rotational field. Reversal in the unidirectional field proceeds by the nucleation and propagation of end domains towards the centre of the granular thin film elements. The formation of a vortex magnetisation structure leads to an increase of the switching time in the granular Co element. The switching time strongly depends on the Gilbert damping parameter α. Small values of α (≤ 0.1) lead to shorter switching times at small field strength values ($h < 0.5\ J_s/\mu_0$). Reversal in rotational fields involves inhomogeneous rotation of the end domains towards the rotational field direction leading to partial flux-closure structures and therefore facilitating the switching by reduced switching times. The micromagnetic study reveals that

switching partly occurs already during the rise time of the unidirectionally oriented external field. Shorter switching times are obtained by the application of a half cycle of a 10 GHz rotational field (t_{sw}=0.05 ns). Precessional oscillation effects after switching off the external field which occurred in the $Ni_{80}Fe_{20}$ square element, were suppressed by the uniaxial anisotropy of the randomly oriented Co grains. Taking into account thermally activated processes the micromagnetic simulations show that the switching time was reduced by less than 10 % at T = 300 K for Co and $H_{ext.}$=140 kA/m (h = 0.1 J_s/μ_0).

Keywords: Numerical micromagnetics,

Precessional switching,

Co nano-elements,

NiFe nano-elements

Corresponding Author:
J. Fidler, Tel: +43 1 58801 13714, Fax +43 1 58801 13798;E-mail: fidler@tuwien.ac.at
Institute of Applied and Technical Physics, Vienna University of Technology,
Wiedner Haupstr. 8-10, A-1040 Wien, Austria.

1. Introduction

The understanding of the magnetic switching behaviour of small particles and thin films becomes increasingly important. Nanoscale magnetic structures with well defined shapes and sizes are of great interest recently due to their potential applications in high density magnetic storage media and spin electronic devices, such as magnetic random access memory [1]. Experimentally, in-situ domain observation using Lorentz electron microscopy, magnetic force microscopy and time resolved magnetic imaging provides a detailed understanding of the domain formation and reversal processes. Numerical micromagnetics is an essential tool to optimise nanostructured magnetic elements for data storage media and sensors. The application of these devices requires a profound knowledge of the reversal mechanism. The basic formalism for magnetic dynamics and switching process is the Landau Lifshitz-Gilbert equation of motion. Experimental and numerical studies have shown that the switching behaviour considerably depends on the damping constant and the shape and size of the nanoelement [2,3,4,5]. Switching times well below 0.5 ns were observed. With decreasing size of the magnetic structures, thermally activated reversal process becomes significant. Thermally induced reversal may influence the writing process as well as the long-term stability of written bits in magnetic recording. Zhang and Fredkin [6] used the finite element method to study thermally activated reversal in ellipsoidal particles large enough to show an inhomogeneous reversal process.

In the present study, three dimensional (3D) micromagnetic simulations of the reversal process within granular nanoscale squares are performed to examine how the switching behaviour of permalloy with zero anisotropy differs from uniaxial Co. Effects of an unidirectional field and a rotational field with variable field strength, field rise time and rotation speed are compared. In addition thermal dynamic effects are discussed for the

granular Co-element. Defects and other forms of disorder as well as eddy currents occurring during the fast switching process are not included in the simulations.

2. Micromagnetic model

The granular thin film element is modelled with columnar grains generated from Voronoi polyhedrons. The polyhedral grains are discretized into tetrahedral finite elements with a constant edge length l_{FE} between 2.5 nm and 5 nm. Previous micromagnetic studies [10,14] have shown that the results are independent of the mesh size, if the finite element size is smaller than the exchange length, which is determined by the stray field

$$l_{ex} = \sqrt{\frac{2\mu_0 A}{J_s^2}}, \qquad (1)$$

or the Bloch parameter

$$\delta_0 = \sqrt{\frac{A}{K_1}}. \qquad (2)$$

Here A is the exchange constant, J_s is the spontaneous magnetic polarisation, and K_1 is the magnetocrystalline anisotropy constant. These length scales determine the width of magnetic inhomogeneities. Generally, the magnetisation will change over a length of πl_{ex} or $\pi\delta_0$ in a Neel wall or Bloch wall, respectively. In order to resolve this transition of the magnetisation, the computational cells have to be smaller than the minimum of l_{ex} and δ_0. Rave and co-workers [7] clearly demonstrated the convergence of the numerical solution, if the cell size becomes smaller than the exchange length.

The basic geometry of the granular thin film element is shown in Fig.1a. The thin, nanostructured square element with dimensions of 100 x 100 x 10 nm^3 consists of 100 irregular shaped grains with an average diameter of about 10nm. For the simulations we used

two sets of materials parameters: The $Ni_{80}Fe_{20}$ nanoelement has the following material properties: J_s=1 T, K_1=K_2=0, A=13 pJ/m. The polycrystalline Co square element consists whether of 3D randomly oriented grains with uniaxial magnetocrystalline anisotropy (Co_3D) or of 2D textured grains with random orientation of the easy axes within the film plane (C_2D). For the simulations the intrinsic bulk properties of hcp-Co were used (J_s=1.76 T, K_1=0.45 MJ/m^3, K_2=0.15 MJ/m^3, A=13 pJ/m).

The micromagnetic simulation method which is based on the Gilbert equation of motion describing the physical path of the magnetic polarisation towards equilibrium was previously explained in detail elsewhere [8]. To solve the Gilbert equation numerically the grains within the nanoelement are divided into tetrahedral finite elements (Fig.1b). The time evolution of the magnetisation at each nodal point of the finite element mesh was calculated using the Gilbert equation. Three different external field profiles (Fig.2) were used for the simulations. In the first case a monotone, increasing "sweep" field with constant sweep rate (2.0 J_s/μ_0 per ns) was uniformly applied along the –y direction until complete magnetisation reversal took place. Second, a homogeneous field was applied after rising the field from zero to h=0.1 and h=0.2 J_s/μ_0 (80 and 160 kA/m for NiFe and 140 and 280kA/m for Co) after 0.05 and 0.10 ns, respectively. Third, in comparison a half cycle (0.05 ns) of a rotating magnetic field with a frequency of 10 GHz was uniformly applied in the (x,y)-plane. A hybrid finite element boundary element method [9] is used to calculate the scalar potential on every node point of the finite element mesh. The demagnetising field, which contributes to the effective field, is the negative derivative of the scalar potential. The effective field $\mathbf{H}_{eff,i}$ at the node point i of an irregular finite element mesh can be approximated using the box scheme. The discretization of the Gilbert equation leads to an ordinary differential equation for every node for each component. The calculations were started from the remanent state after saturation parallel to the y-direction. The simulations were terminated at $J_y < 0.9\ J_s$: Previous micromagnetic

simulations have shown that the damping parameter α strongly influences the switching time [10]. Shorter switching times are obtained at low external field strength values ($h < 0.5\ J_s/\mu_0$). In the present study the Gilbert damping parameter was kept constant to α=0.1. Due to the small size, eddy currents are considered to be small and therefore are neglected.

The theoretical treatment of thermal process on the small time scale usually starts from the Langevin equation [6,11,12]. Although the details of the implementations differ, all authors [6,11,12] apply the fluctuation dissipation theorem in order to derive the strength of a random thermal field which is then added to the effective field in the Gilbert equation of motion. Thermal activations on a short time scale can be treated numerically adding a stochastic thermal fluctuation field to the effective magnetic field in the Gilbert equation of motion, leading to the Langevin equation [13]:

$$\frac{d\mathbf{J}}{dt} = -|\gamma_0|\mathbf{J}\times\left(\mathbf{H}_{eff} + \mathbf{H}_{th}\right) + \frac{\alpha}{J_s}\mathbf{J}\times\frac{\partial\mathbf{J}}{\partial t} \qquad (3)$$

At each time step, which is in the order of fs, the effective field term $\mathbf{H}_{\mathrm{eff}}$ include the applied field, the exchange field, the magneto-crystalline anisotropy field and the demagnetising field. The term γ_0 is the gyromagnetic ratio of the free electron spin and α is the damping constant. The first term on the right hand side of equation (3) accounts for the gyromagnetic precession of the magnetic polarization **J**, the second term arises from viscous damping. The thermal field is assumed to be a Gaussian random process with the following statistical properties: At high damping the magnetisation rotates more or less directly towards the field direction, as the second term is dominant. If the precession term becomes dominant, the polarisation precesses several times around the field direction before it reaches equilibrium. Finally low damping and finite temperatures causes a random motion of the magnetisation in thermal equilibrium. The resulting stochastic equation of motion describes the random motion of the magnetisation in thermal equilibrium and eventually across energy barriers. The random thermal field, $\mathbf{H}_{\mathrm{th}}$,

describes the coupling of the magnetic system with a heat bath. It accounts for the interaction of the magnetic polarisation with the microscopic degrees of freedom which causes the fluctuation of the magnetisation distribution. The fluctuations are assumed to take place on a much faster time scale than the intrinsic time scale given by the gyromagnetic ratio and the effective field. The average of the thermal field taken over different realizations vanishes in each direction in space. The thermal field is uncorrelated in time and uncorrelated at different node points of the finite element mesh. The strength of the thermal fluctuation field H_{th} follows from the fluctuation-dissipation theorem [12] and is given by:

$$H_{th} = \sqrt{\frac{2\alpha k_B T}{\Delta t \gamma J_s l^3}}. \qquad (4)$$

where Δt is the time step of the time integration method, k_B is the Boltzmann constant, T the temperature and l_{FE} is the mesh size of the finite element grid.

At zero temperature the interplay between exchange interactions and the demagnetising field or the interplay between exchange and magnetocrystalline anisotropy causes the magnetisation to change its direction over a length given by πl_{ex} or $\pi\delta_0$. At finite temperature thermal noise may cause the magnetisation to rotate out of its preferred orientation. This will cause a change of the magnetisation not only on the lattice site where the magnetisation was randomly kicked by the thermal field but also in its surroundings. The fluctuation of the magnetisation due to the thermal event extends over a characteristic length which is now governed by the interplay between the exchange interactions and the strength of the thermal field. We can define a thermal exchange length [14]

$$l_{thex} = \sqrt{\frac{A}{J_s H_{th}}}, \qquad (5)$$

The thermal exchange length decreases with increasing temperature but also depends on the Gilbert damping constant, the time step, and the cell size. From equations (4) and (5) it is

obvious that the calculated switching properties are independent of the cell size, if the l_{FE} is smaller than the thermal exchange length.

3. Results and Discussion

To study the effect of the applied field on the magnetisation reversal process different sets of material parameters have bee used in the simulations. As result of the numerical calculations of the switching behaviour of the $Ni_{80}Fe_{20}$ and the hcp-Co granular square element it is found that fastest switching ($<J_y>=0$) occurs at lowest magnetic field values in the case of zero anisotropy. Figure 3 compares the time evolution of the polarisation of $Ni_{80}Fe_{20}$ with randomly oriented (Co_3D) and in plane textured(Co_2D) Co grains, if the uniform field is applied along the –y direction under a constant sweep rate of 2.0 J_s/μ_0 per ns. The oscillations of the polarisation after abruptly switching off the field indicate that precessional effects occur in NiFe exiting a resonance. A pronounced switching is found in the granular Co thin film element, whereas the 3D randomly oriented grains lead to a slightly faster switching process compared to the 2D textured element. The magnetisation of the elements was completely reversed at an external field of 263 kA/m and 532 kA/m for the NiFe and the Co_3D square, respectively. The diagrams of Fig.4 compare the time evolution of the polarisation component parallel to the applied field J_y for different field profiles *H(t)*, i.e unidirectional field after a field rise from zero and rotational field, and maximum field strength values for the $Ni_{80}Fe_{20}$ thin film element.. It obvious that the precessional oscillation effects of the polarisation vector increase with a larger field value (h=0.2 J_s/μ_0) and are more pronounced after switching off the high frequency rotational field at t=0.05 ns (Fig.4b). Despite the shorter switching time obtained by the rotational field the precessional instability hinders the square $Ni_{80}Fe_{20}$ element from a clear switching behaviour.. For the static field cases and the rotational field at h=0.1 J_s/μ_0 switching times less than 0.1 ns were calculated neglecting thermal activation processes.

The numerical simulations show that in the NiFe square with zero magnetocrystalline anisotropy the reversal process starts from the remanent state by rotating the magnetisation in the end domains within the square during the rise time, if the field is applied uniformly parallel to the –y direction. Figure 5a shows the transient magnetisation state after 0.036 ns (J_y= 0.66 J_s). In contrary, the reversal process by the application of the rotational field of 80 kA/m leads only to an overall decrease of J_y to a value of 0.5 J_s, thus the complete reversal takes place after switching off the field (Fig. 4a). Figure 5b shows the magnetisation pattern just after switching off the rotational field (t=0.062 ns, J_y = 0). The reversal starts in the centre of the element, whereas the magnetisation in the regions along the square edges parallel to the x-direction only partly reversed. The out of plane components of the polarisation vector during the reversal should be noted (Figs.5a and b).

The micromagnetic simulations reveal that the switching mechanisms differ from the ones of $Ni_{80}Fe_{20}$, if the uniaxial anisotropy of the randomly oriented Co grains is taken into account. The comparison of the time evolution of the polarisation of the granular Co square during the application of an uniform field and a rotating field at 10 GHz shows in Fig.6 that the complete switching already occurred after switching off the rotational field for both H_{ext}= 140 kA/m (h=0.2 J_s/μ_0) and H_{ext}= 280 kA/m (h=0.2 J_s/μ_0). A switching time > 0.2 ns was found after the application of a uniform field with a field rise time of 0.05 ns and a field strength value of h=0.1 J_s/μ_0 (Fig.6a). Faster switching occurred, if the field strength was increased to h=0.2 J_s/μ_0 (Fig.6b). The transient magnetisation state of Fig.7a during switching (<J_y=0>) for h=0.2 J_s/μ_0 and at t=0.095 ns indicates that switching occurred after nucleation and expansion of reversed domains starting from two opposite corners of the granular element. On the other hand inhomogeneous magnetisation rotation processes are dominant and lead the complete switching of the element under the influence of a constant, half cycle rotating field of 10 GHz. As shown in Fig. 7b the magnetisation tries to follow the applied field direction and starts to

rotate nearly in all grains at h=0.2 J_s/μ_0 and t=0.031 ns(<J_y=0>). Precessional oscillation effects which occurred in the NiFe square, were obviously suppressed by the uniaxial anisotropy of the randomly oriented grains. We observed that the switching time decreases by a factor of about 10%, if a 3D random orientation of the grains is assumed compared to a 2D texture within the film plane.

Taking into account thermally activated processes the micromagnetic simulations show that the switching time slightly decreases at elevated temperature, such as T=300 K (Fig.8a). According to equations (4) and (5) suitable sizes for the finite element mesh and time step were chosen. For simplicity of these simulations no field rise time was considered and the field of h=0.1 J_s/μ_0 was instantaneously applied along the –y direction. The numerical simulations started from the remanent state of the thin film Co_3D element. The magnetisation pattern of Fig.8b clearly shows that the formation of a twin-vortex like structure at t=0.30 ns(<J_y=0>). hinders the fast switching of the element, especially at a low applied field strength value.

4. Conclusions

A 3D micromagnetic model was used to simulate the influence of different applied field profiles and field strength values up to 0.2 J_s/μ_0 on the magnetisation reversal processes of a thin, granular square element of 100x100x10 nm^3 and assuming a damping parameter of α=0.1. It has been shown that rotational applied fields of 10 GHz reveal only a partial inhomogeneous rotation in a NiFe square with zero anisotropy and show a precessional oscillation effect of the polarisation after abruptly switching off the field. Rotational fields considerably decrease the switching time to < 0.05 ns in a randomly oriented polycrystalline Co square with about 10 nm grain size. Unidirectional applied fields lead to an

inhomogeneous magnetisation rotation within the NiFe square, whereas in the polycrystalline Co-element the formation of vortex domain structures considerably increases the switching time. Thermal dynamic effects are found to influence the switching process and to slightly decrease the switching times, if zero temperature simulations obtained switching times larger than 0.3 ns.

Acknowledgements

This work was supported by the Austrian Science Fund (P13260-TEC and Y-132 PHY).

References

[1] St. Y. Chou, IEEE Trans Magn. 85 (1997) 652.

[2] W. Wernsdorfer, E.B. Orozco, B. Barbara, K. Hasselbach, A. Benoit, D. Mailly, B. Doudin, J. Meier, J.E. Wegrowe, J.P. Ansermet, N. Demoncy, H. Pascard, L. Francois, N. Duxin and M.P. Pileni, J. Appl. Phys. 81 (1997) 5543.

[3] R. Kikuchi, J. Appl. Phys. 27 (1956) 1352.

[4] T. Leineweber and H. Kronmüller, J. Magn. Magn. Mater. 192 (1999) 575.

[5] R. H. Koch, Phys. Rev. Lett. 81 (1998) 4512.

[6] K. Zhang and D. R. Fredkin, J. Appl. Phys. 85 (1999) 5208.

[7] W. Rave, K. Ramstock and A. Hubert, J. Magn. Magn. Mater. 183 (1998) 329.

[8] J. Fidler and T. Schrefl, J. Phys. D 33 (2000). R135.

[9] D. R. Fredkin and T. R. Koehler, IEEE Trans. Magn. 26 (1990). 415.

[10] J. Fidler, T. Schrefl, V. D. Tsiantos, W. Scholz and D. Suess, J. Computational Physics, (2001) in press.

[11] Y. Nakatani, Y. Uesaka, N. Hayashi, and H. Fukushima, J. Magn. Magn. Mater. 168 (1997) 347.

[12] J. L. Garcia-Palacios and F. J. Lazaro, Phys. Rev. B 58 (1998) 14937.

[13] W Scholz, T. Schrefl and J. Fidler, J. Magn. Magn. Mat., 233 (2001) 296.

[14] V. Tsiantos, W. Scholz, D. Suess, T. Schrefl and J. Fidler, J. Magn. Magn. Mater. (2002) in press-

Figure Captions

Fig.1. (a) Schematic geometry of granular structure of a square thin film element with the dimensions of 100 x 100 x 10 nm^3 consisting of 100 grains with a grain size of about 10 nm. (b) Discretization into tetrahedral finite elements used for the numerical simulation.

Fig.2. Different profiles of the applied field (H(t) along to the –y direction were used for the numerical simulations. (a) A monotone, increasing "sweep" field with a constant sweep rate (2.0 J_s/μ_0 per ns) is applied until switching occurs. (b) The uniform static field is applied after rising the field from zero to h=0.1 or 0.2 J_s/μ_0. (c) The rotating uniform magnetic field with a frequency of 10 GHz and a field strength value of h=0.1 or 0.2 J_s/μ_0 is applied in the (x,y)-plane and is switched off after a half cycle of rotation (0.05 ns).

Fig. 3. Comparison of the time evolution of the polarisation parallel to the field direction during the application of a "sweep" field for NiFe with zero anisotropy, uniaxial Co with random 3D orientation of the grains (Co_3D) and 2D in plane texture (Co_2D).

Fig. 4. Time evolution of the polarisation of the $Ni_{80}Fe_{20}$ square element during the application of a unidirectional field after field rise and a half cycle of a rotating field at 10 GHz (rot) for (a) H_{ext}= 80 kA/m (h=0.1 J_s/μ_0) and (b) H_{ext}= 160 kA/m (h=0.2 J_s/μ_0).

Fig. 5. Transient magnetisation states within the $Ni_{80}Fe_{20}$ square during the reversal process for H_{ext}=80 kA/m (h=0.1 J_s/μ_0) occurring (a) in an uniformly applied field at t=0.0.036 ns with $<J_y>$= 0.66 J_s and (b) shortly after the application of a half cycle of a 10GHz rotational field at t=0.062 ns with $<J_y>$= 0.

Fig. 6. Time evolution of the polarisation of the granular Co_3D square element during the application of a unidirectional field after field rise and a half cycle of a rotating field at 10 GHz (rot) for (a) H_{ext}= 140 kA/m (h=0.1 J_s/μ_0) and (b) H_{ext}= 280 kA/m (h=0.2 J_s/μ_0).

Fig. 7. Transient magnetisation states within the granular Co_3D square during the switching process (<J_y>= 0) for H_{ext}=280 kA/m (h=0.2 J_s/μ_0) occurring (a) in an uniformly applied field at t=0.0.095 ns and (b) during the application of a half cycle of a 10GHz rotational field at t=0.031 ns.

Fig. 8. (a) Taking into account thermally activated processes the micromagnetic simulations show that a decrease of the switching field of the Co square at an elevated temperature(T=300 K). Reversal starts from the remanent state after an instantaneously applied field of h=0.1 J_s/μ_0.. (b) The magnetisation pattern during switching at t=0.30 ns(<J_y=0>) show the formation of a twin-vortex like structure.

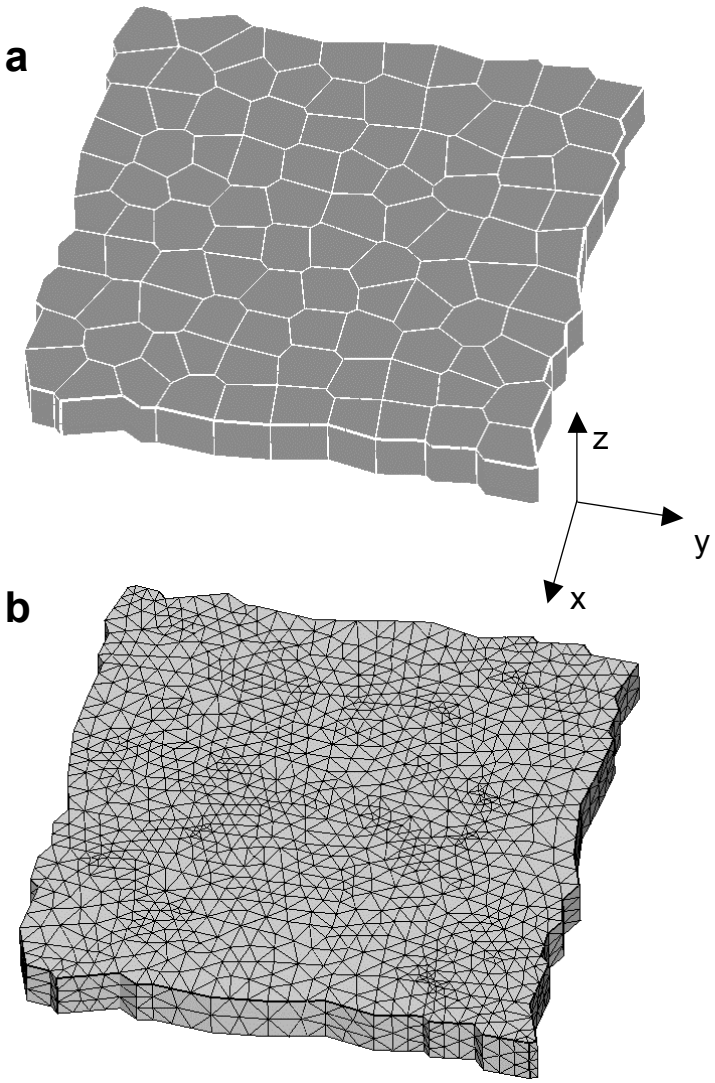

Fig. 1

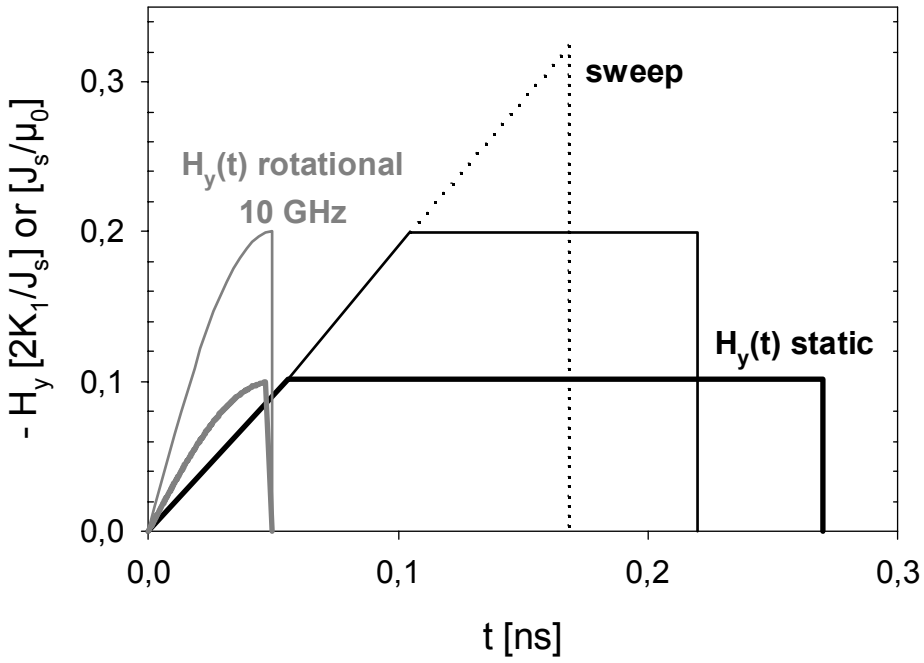
sweep
H_y(t) rotational
10 GHz
H_y(t) static
- H_y [$2K_1/J_s$] or [J_s/μ_0]
t [ns]
0,0
0,1
0,2
0,3

Fig. 2

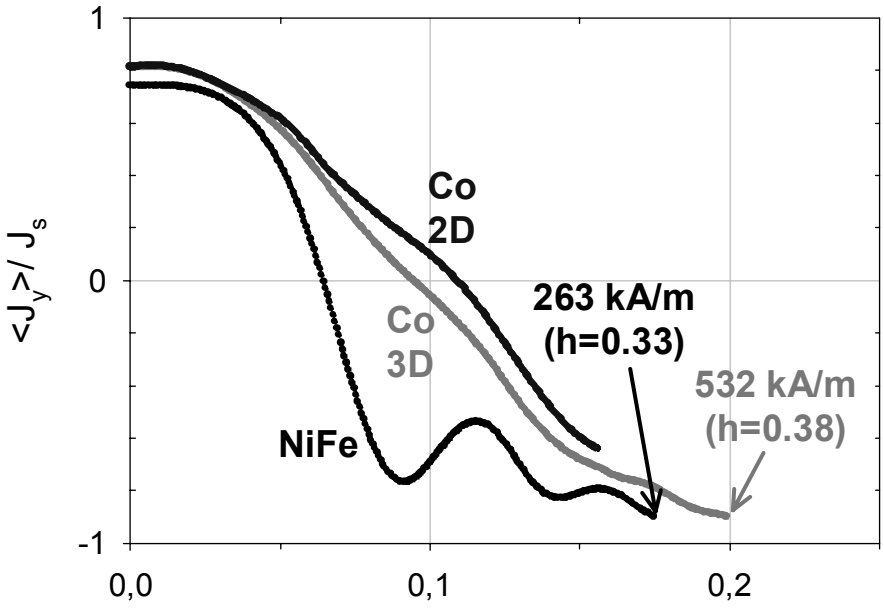

Fig. 3

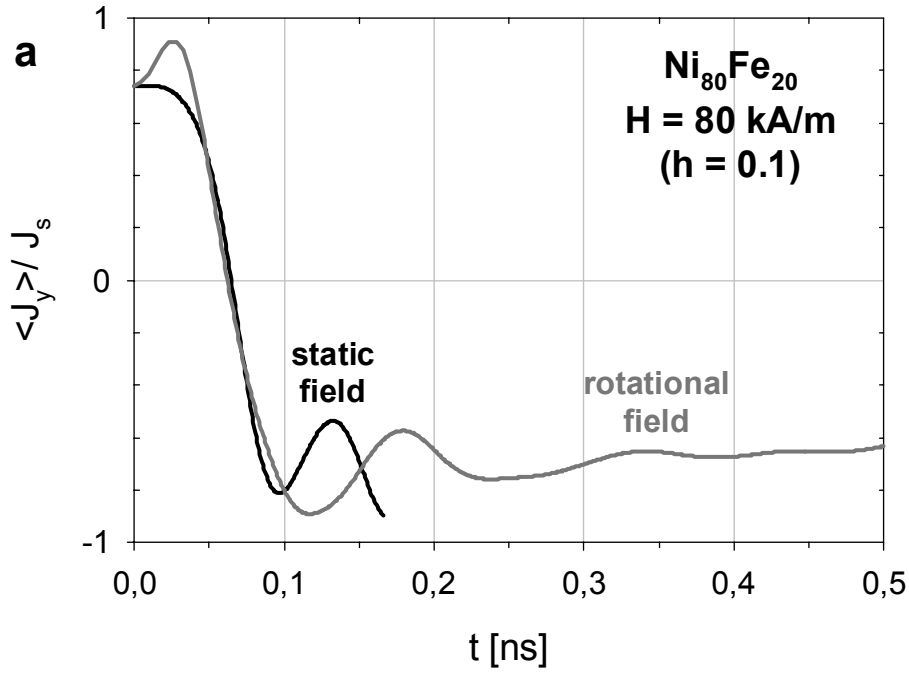
a
Ni80Fe20
H = 80 kA/m
(h = 0.1)
static
field
rotational
field
<Jy>/ Js
1
0
-1
0,0
0,1
0,2
0,3
0,4
0,5
t [ns]

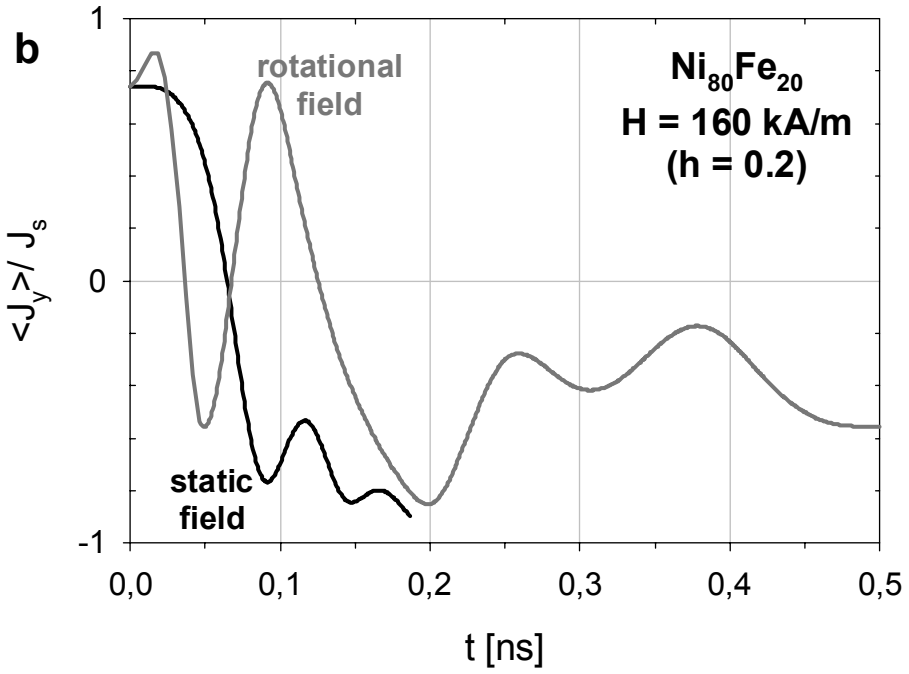
b
rotational
field
Ni80Fe20
H = 160 kA/m
(h = 0.2)
static
field
<Jy>/ Js
1
0
-1
0,0
0,1
0,2
0,3
0,4
0,5
t [ns]

Fig. 4

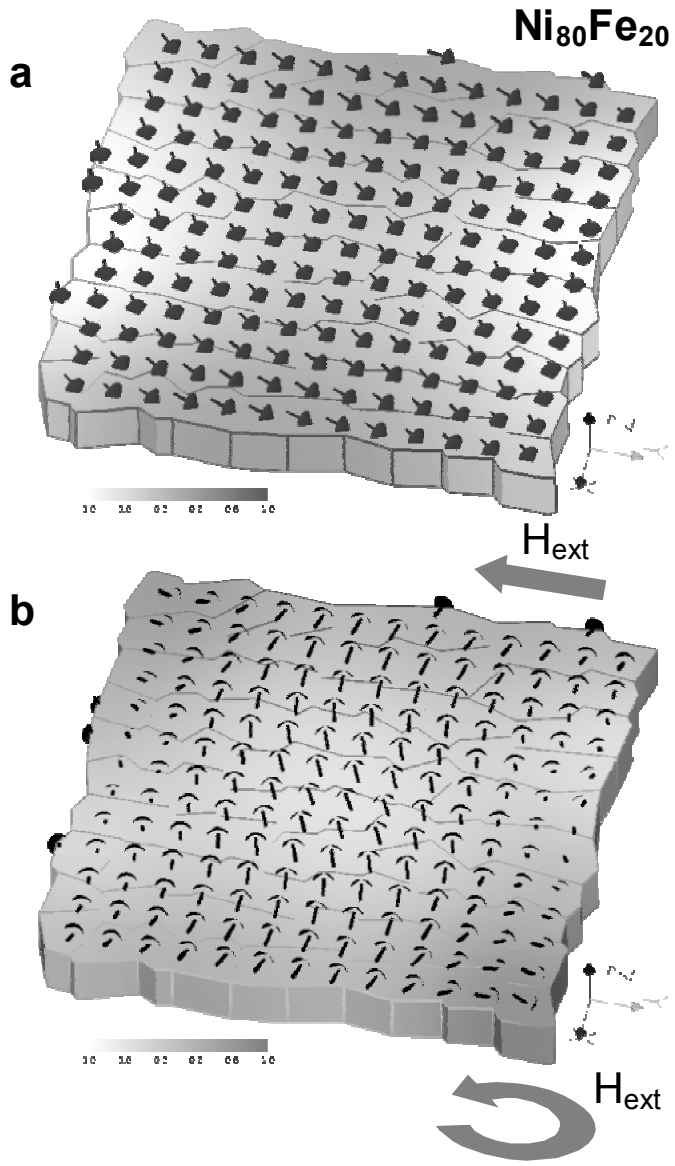

Fig. 5

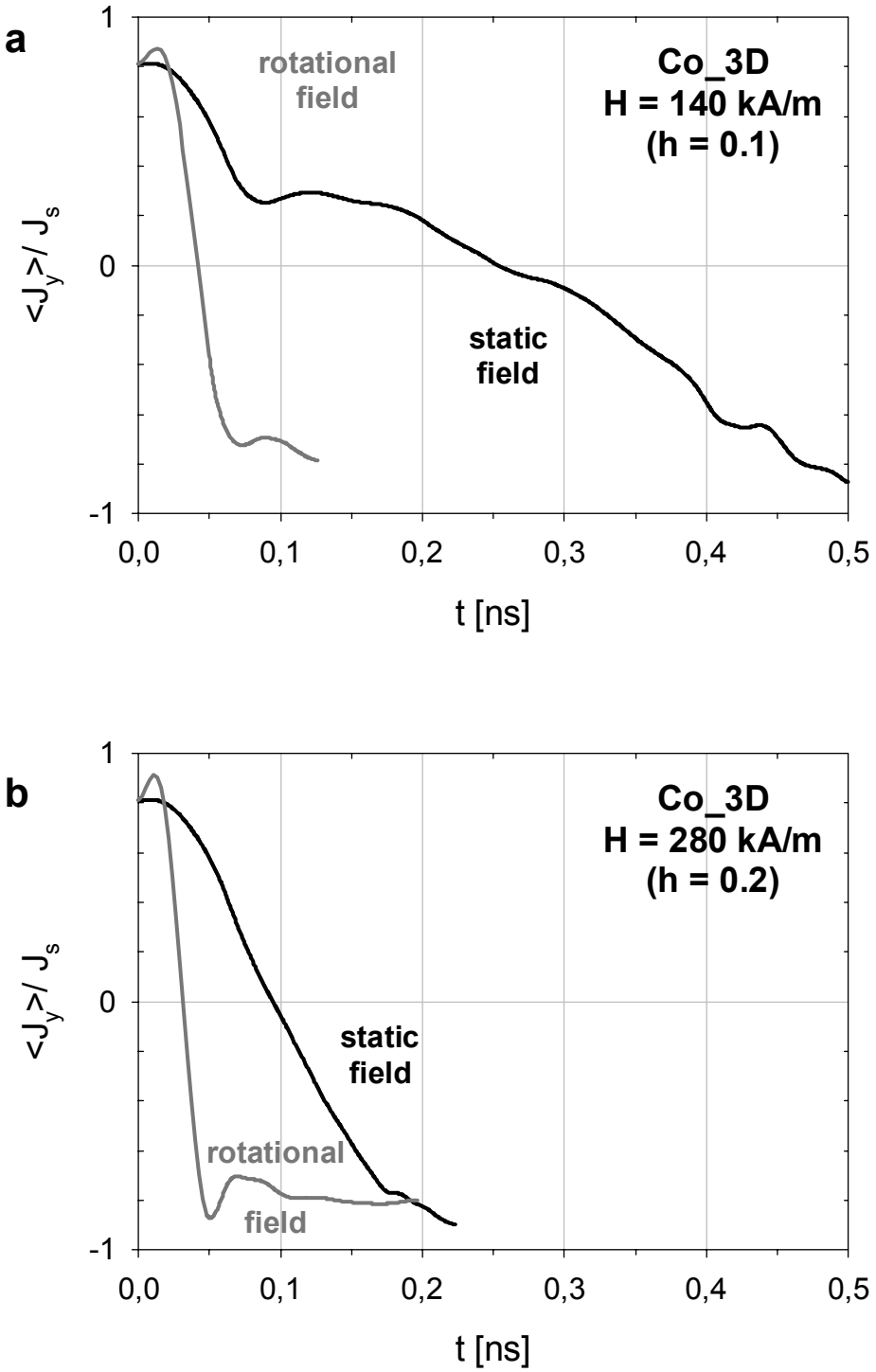
a
rotational
field
Co_3D
H = 140 kA/m
(h = 0.1)
static
field
<J_y>/ J_s
1
0
-1
0,0
0,1
0,2
0,3
0,4
0,5
t [ns]
b
Co_3D
H = 280 kA/m
(h = 0.2)
static
field
rotational
field
<J_y>/ J_s
1
0
-1
0,0
0,1
0,2
0,3
0,4
0,5
t [ns]

Fig. 6

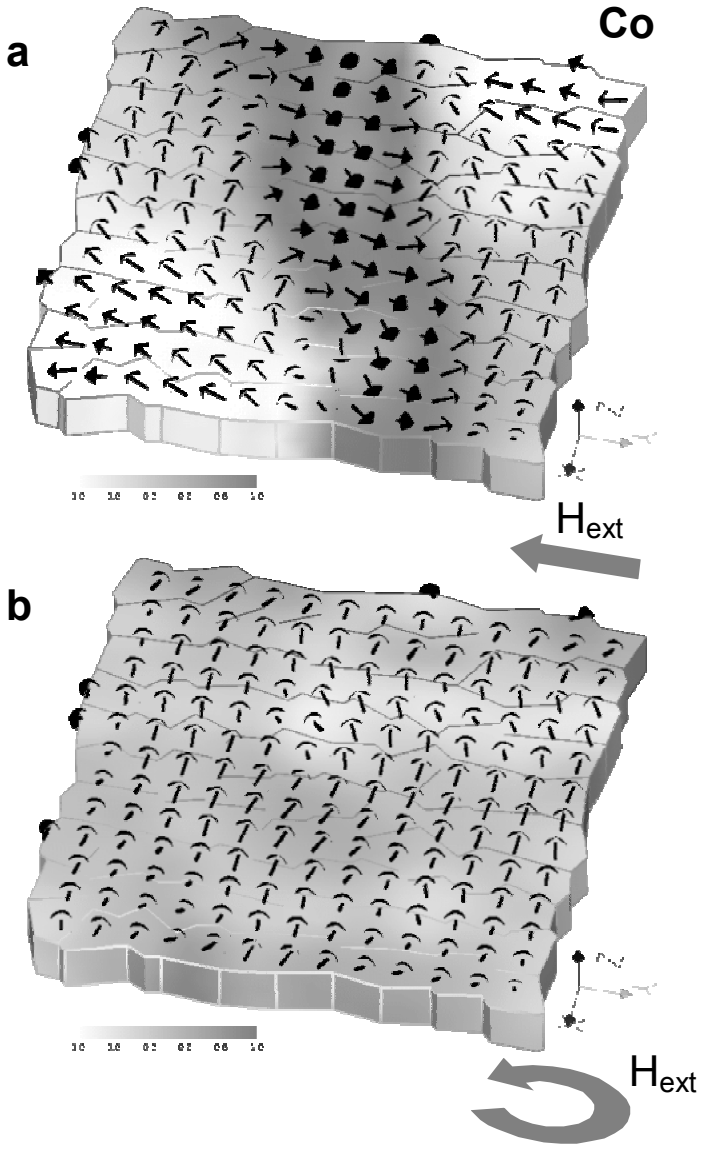

Fig. 7

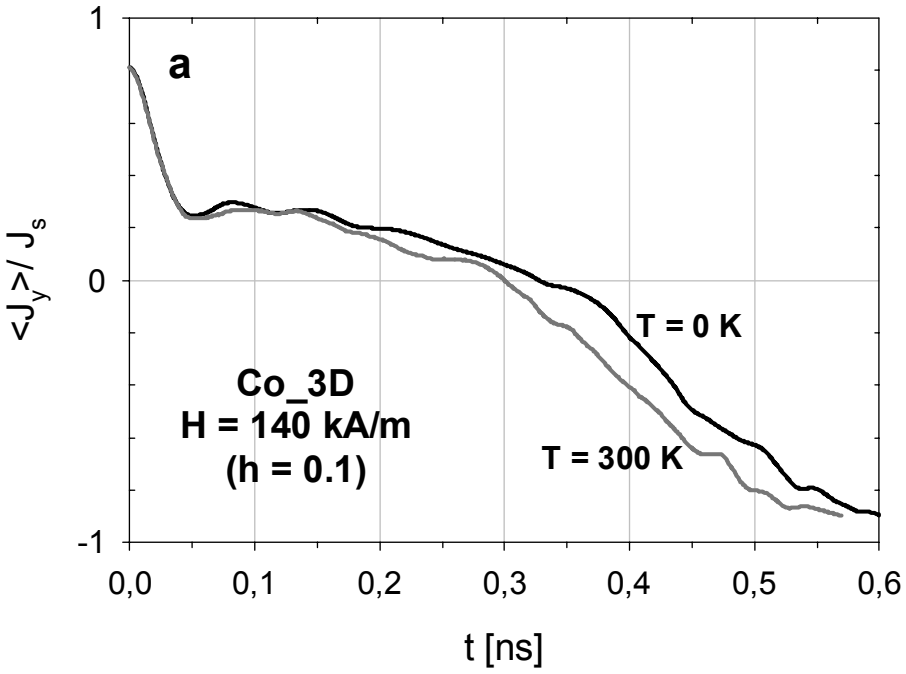
a
1
0
-1
<J_y> / J_s
T = 0 K
T = 300 K
Co_3D
H = 140 kA/m
(h = 0.1)
0,0
0,1
0,2
0,3
0,4
0,5
0,6
t [ns]

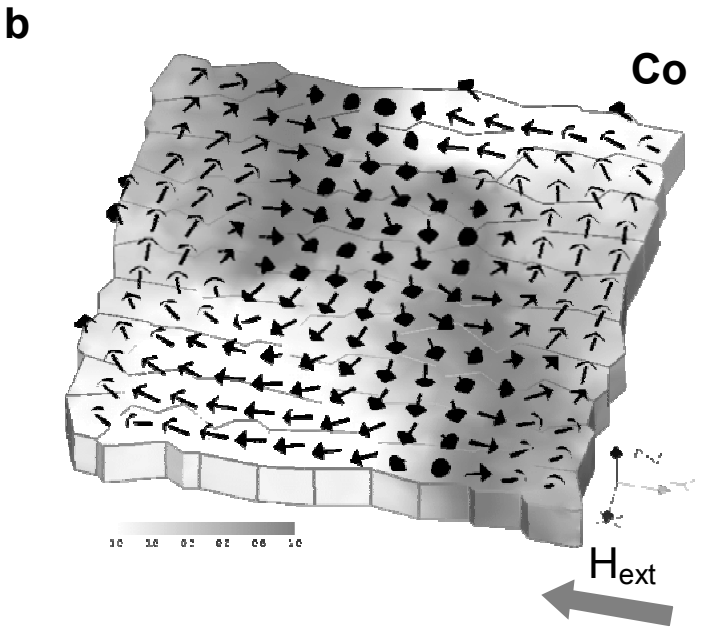
b
Co
H_ext

Fig.8